

Bachelorarbeit

Jesslyn Callista Wijaya

Design and Implementation of a Solderless Measurement
Environment for Characterizing Common Mode Chokes

Jesslyn Callista Wijaya

Design and Implementation of a Solderless Measurement Environment for Characterizing Common Mode Chokes

Bachelor thesis submitted for examination in Bachelor's degree
in the study course *Bachelor of Science Elektro- und Informationstechnik*
at the Department Information and Electrical Engineering
at the Faculty of Engineering and Computer Science
at University of Applied Science Hamburg

Supervisor: Prof. Dr. Frerk Haase
Supervisor: Prof. Dr. Martin Lapke

Submitted on: 9. September 2024

Jesslyn Callista Wijaya

Thema der Arbeit

Entwurf und Implementierung einer lötfreien Messumgebung zur Charakterisierung von Gleichtaktdrosseln

Stichworte

Gleichtaktdrosseln, Vektor-Netzwerkanalysator, S-Parameter, 3D-Druck, Relative Permittivität

Kurzzusammenfassung

Diese Studienarbeit zielt darauf ab, einen neuen Ansatz zur Charakterisierung einer Gleichtaktdrossel mithilfe einer 3D-gedruckten Halterung zu entwickeln, die das Löten überflüssig macht.

Jesslyn Callista Wijaya

Title of Thesis

Design and Implementation of a Solderless Measurement Environment for Characterizing Common Mode Chokes

Keywords

Common Mode Chokes, Vector Network Analyzer, S-Parameters, 3D Print, Relative Permittivity

Abstract

This thesis aims to develop a different approach for characterizing a common mode choke using a 3D printed fixture, eliminating the need for soldering.

Contents

List of Figures	vi
List of Tables	viii
Abbreviations	ix
1 Introduction	1
2 Theory	2
2.1 Common mode choke	2
2.2 Mixed-mode S-Parameter	3
2.3 3D filaments	5
2.3.1 Relative permittivity (ε_r) of 3D filaments	6
3 Setup and Limits	8
3.1 Test setup and parameters	8
3.1.1 3D design, slicing and printing	9
3.1.2 Test fixtures design	10
3.2 Recommended limits	12
4 Test execution and evaluation	14
4.1 Calibration	14
4.2 Measurement and evaluation	15
4.2.1 Mechanical pressure	15
4.2.2 Inlay	18
4.2.3 Material	20
4.2.4 Validation	23
4.2.5 Verification	28
5 Conclusion and future work	34

Contents

A Appendix	38
A.1 Tools and Equipment	38
Declaration of Authorship	39

List of Figures

2.1	Common mode choke [13]	3
2.2	Magnetic flux behaviour in CMC[1]	3
2.3	Mixed-mode S-parameter [14]	4
3.1	CMC test board	8
3.2	Test setup for S-Parameter measurements [2]	9
3.3	The initial state	10
3.4	First version	10
3.5	Second version	11
3.6	Final version	12
3.7	Recommended limit for S_{dd11} and S_{dd22} (RL) [2]	12
3.8	Recommended limit for S_{dd21} (IL) [2]	13
3.9	Recommended limit for S_{cc21} (CMR) [2]	13
4.1	Calibration board	15
4.2	Pressure test - S_{dd11}	16
4.3	Pressure test - S_{dd22}	16
4.4	Pressure test - S_{dd21}	17
4.5	Pressure test - S_{cc21}	17
4.6	Inlay test - S_{dd11}	18
4.7	Inlay test - S_{dd22}	19
4.8	Inlay test - S_{dd21}	19
4.9	Inlay test - S_{cc21}	20
4.10	Material test - S_{dd11}	21
4.11	Material test - S_{dd22}	21
4.12	Material test - S_{dd21}	22
4.13	Material test - S_{cc21}	22
4.14	Validation test - S_{dd11}	24
4.15	Validation test - S_{dd22}	25

4.16 Validation test - S_{dd21}	26
4.17 Validation test - S_{cc21}	27
4.18 Verification test - S_{dd11}	29
4.19 Verification test - S_{dd22}	30
4.20 Verification test - S_{dd21}	31
4.21 Verification test - S_{cc21}	32

List of Tables

4.1	Calibration parameters [6]	14
A.1	Tools and equipment	38

Abbreviations

.stl Stereolithography.

ABS Acrylonitrile-Butadiene-Styrene.

CMC Common Mode Choke.

CMR Common Mode Rejection.

DUT Device Under Test.

EMC electromagnetic compatibility.

EMI electromagnetic interference.

ESD electrostatic discharge.

IL Insertion Loss.

PCB Printed Circuit Board.

PETG Polyethylene Terephthalate Glycol.

PLA Polylactic Acid.

RL Return Loss.

S-Parameters Scattering Parameters.

TOSM Through, Open, Short, Match.

VNA Vector Network Analyzer.

1 Introduction

The Common Mode Choke (CMC) is a crucial component in communication networks, essential for meeting electromagnetic compatibility (EMC) requirements. It functions by filtering out unwanted common-mode noise while allowing the differential signal to pass through. Ensuring accurate EMC measurements require that CMCs function properly, as they play a key role in reducing electromagnetic interference (EMI). The main challenge lies in the significant variation between CMC samples. To accurately determine the S-parameters of the specific CMC being used, it must be measured before deployment. However, this requires a special test board, and the process of de-soldering carries the risk of damaging the CMC, which can alter the characteristics.

The goal of this thesis is to introduce a different approach that eliminates the need for soldering by utilizing a 3D-printed fixture. 3D printing was chosen due to its suitability for rapid prototyping, low production cost and consistent reproducibility of results. This method simplifies the testing process, also ensuring that CMCs can be tested accurately without compromising their integrity or complicating their replacement and reuse.

The proposed fixture is designed to sit on top of a standardized Printed Circuit Board (PCB) from FTZ Zwickau, specifically designed for characterizing the CMC. By enabling direct measurement of mixed-mode Scattering Parameters (S-Parameters) with the help of a Vector Network Analyzer (VNA), this setup facilitates accurate and repeatable characterization of the CMC. Furthermore, the design of the 3D fixture incorporates configuration that have been carefully selected to enhance ease of use while minimizing external influences such as mechanical stress or movement, which could otherwise compromise the integrity of the measurements. These considerations make the fixture not only a practical tool for laboratory settings but also a reliable method for achieving high-precision measurements, ultimately improving the process of CMC characterization.

2 Theory

2.1 Common mode choke

Common mode chokes are electrical filters used in power and signal circuits to block unwanted high-frequency noise signal (common mode noise) while allowing the desired signals (differential signal) to pass. Common mode noise often originates from external sources such as radio frequency interference, unshielded electronics, or nearby electrical devices. If not properly filtered, this noise can cause EMI, which is unwanted and can disrupt the proper functioning of electronic circuits.

There are two types of CMC. The first type features solid iron cores with high saturation and current ratings, making them suitable for suppressing noise in the audio frequency range (up to 30kHz) and commonly used in power circuits. The second type utilizes ferromagnetic core and rated for lower current application, designed to address higher frequency noise (above 30kHz), which is used in signal circuits [1]. Both types incorporate two coils with multiple windings that are connected. In this case, the CMC being characterized is TDK ACT1210L-201-2P-TL00 for Ethernet, which is used in a signal circuit.

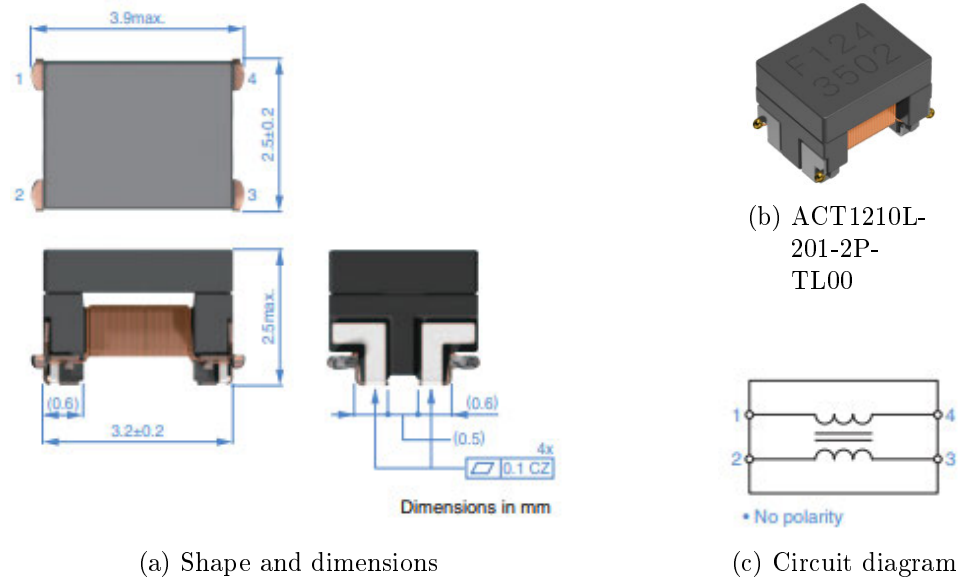


Figure 2.1: Common mode choke [13]

When common mode noise tries to pass through, the CMC generates magnetic flux in both coils, creating a magnetic field that blocks the noise, especially at high frequencies, while allowing lower frequencies to pass (Figure 2.2a). In contrast, when the actual signal, which flows in opposite direction (differential signal) goes through, the magnetic fields cancel each other out, allowing the signal to pass through with little resistance (Figure 2.2b). This helps maintain the signal quality without letting noise interfere.

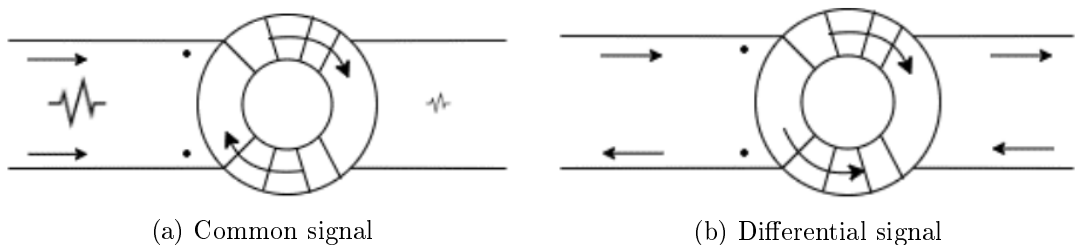


Figure 2.2: Magnetic flux behaviour in CMC[1]

2.2 Mixed-mode S-Parameter

One way to characterize a CMC is to measure mixed mode S-parameters using a VNA. S-parameters are used to measure the amount of signal that successfully transmits through

a Device Under Test (DUT) and the amount that bounces back at high frequencies like radio and microwave frequency, while mixed-mode S-parameters are used when a device handles both single-ended signals (one signal at a time) and differential signals (two complementary signals). They help in analyzing how both types of signals are affected by the device.

A 4-port DUT has 16 S-parameters, divided into four quadrants containing differential-mode, common-mode and cross-mode S-parameters shown in Figure 2.3a. Figure 2.3b shows the notation for S-parameters, where the "xx" indicates the signal type, using "D" for differential and "C" for common signal. The numbers represent the input or output port, with the first number indicating the output port and the second representing the input port.

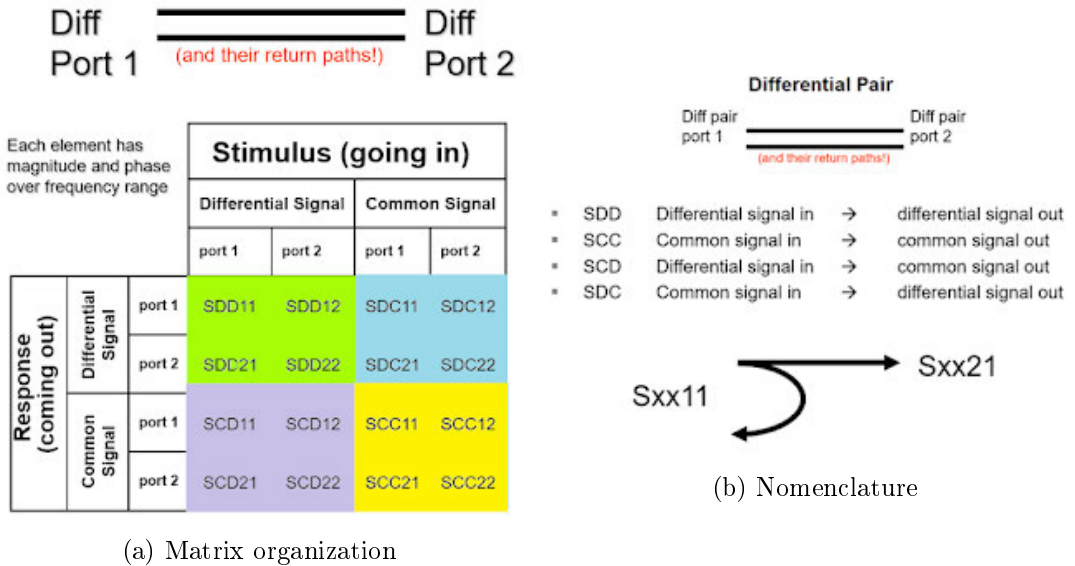


Figure 2.3: Mixed-mode S-parameter [14]

The relevant S-parameters for a 4-port measurement for this thesis are S_{dd11} , S_{dd22} , S_{dd21} and S_{cc21} , where:

- S_{dd11} : Differential mode reflection at port 1, also known as input Return Loss (RL),
- S_{dd22} : Differential mode reflection at port 2, also known as output RL,
- S_{dd21} : Differential mode transmission from port 1 to port 2, also known as input Insertion Loss (IL),

- S_{cc21} : Common mode transmission from port 1 to port 2, also known as input Common Mode Rejection (CMR).

RL indicates the amount of power that is reflected back to the source due to a load mismatch and is defined in decibels (dB). A high RL is desirable, as it indicates that only a small portion of the signal is reflected, leading to better device performance. Low RL suggests a poor impedance match, that can lead to reduced performance or data errors.

IL measures how much of the signal is lost as it passes through a device, also expressed in decibels (dB). The signal attenuation occurs for any type of transmission, whether it's electricity or data. Unlike RL, where higher values are preferable, lower IL values are better. Generally, a lower IL is associated with a higher RL.

CMR measures how effectively a device can reject unwanted noise. A high CMR indicates that the device is effective at suppressing noise that could interfere with the signal, ensuring a good signal quality.

2.3 3D filaments

The market for 3D filaments is highly diverse, with each type of filament suited to different applications. Polylactic Acid (PLA), Acrylonitrile-Butadiene-Styrene (ABS) and Polyethylene Terephthalate Glycol (PETG) are the most commonly used and readily accessible.

PLA is the most frequently used material for 3D printing, made from renewable resources like sugarcane or cornstarch. It is very easy to print with, which is why it is very popular among beginners. PLA is known for minimal warping and provides smooth finish. It requires a relatively low printing temperature of around $180 - 220^{\circ}\text{C}$ [11], which also results in the finished print having lower heat resistance.

ABS is a thermoplastic known for its strength and durability. It requires a higher printing temperature of around $220 - 260^{\circ}\text{C}$ [11] and thereby is heat resistant. However, ABS is prone to warping, making it more challenging to print with. To prevent the material from pulling away from the print bed, it's recommended to apply a layer of glue to the bed when printing with ABS.

PETG is a popular choice for outdoor application due to its UV resistance. It is durable, strong and chemical resistant but unfortunately not moisture resistant. PETG must be stored in a dry environment as it easily absorbs moisture from the air, which can cause issues during printing. This can be remedied by drying the filament at around 65°C for at least 2 hours. PETG require a high printing temperature between 220 – 250°C [11]. One common issue with PETG is stringing, which can result in a "hairy" finish on prints.

2.3.1 Relative permittivity (ε_r) of 3D filaments

Since the CMC will be held in place by the fixture, the relative permittivity of the fixture becomes an important factor to consider. A material with high relative permittivity can alter the distribution of electric fields, potentially affecting how well a device can shield or filter EMI. The goal is to achieve a relative permittivity as low as possible, ideally as close to that of air, which is approximately 1.0005 [4] at standard room temperature and atmospheric pressure. This is essential for maintaining signal integrity, especially in communication devices. Determining the exact value of the relative permittivity for these three filaments can be challenging, because these values are influenced by various factors, including frequency, infill density, infill pattern and even color, among others. But it is known that each filament has a distinct relative permittivity.

Infill density and infill pattern both influence relative permittivity and are interdependent. Logically, lower infill densities result in lower relative permittivity due to the increased presence of air pockets. According to a 2023 paper, at lower infill densities, the geometry of the infill affects relative permittivity. However, at a maximum infill density, the infill geometry has no impact on relative permittivity. The study also reveals that different patterns affect materials differently; for PLA, the corrugated pattern performs best at lower density, whereas for ABS, the square pattern is most effective [5].

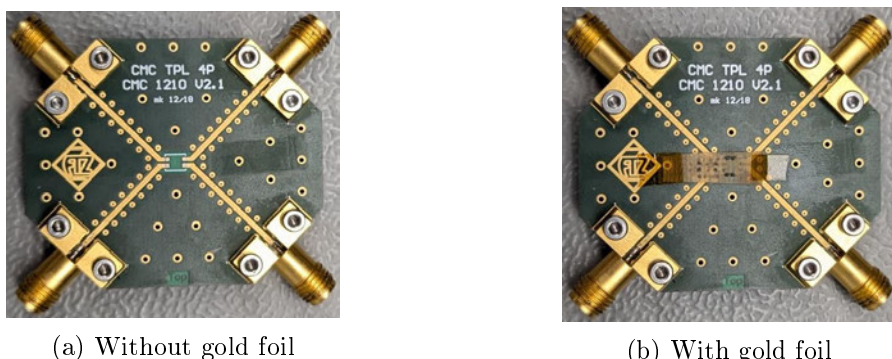
Another factor mentioned is color. According to Picha et al. [7], colored and colorless versions of the same material have different values of relative permittivity. They tested PLA in three colors: transparent, silver, and metallic green. While the transparent and silver samples showed similar relative permittivity, the metallic green sample had a higher permittivity. This indicates that certain pigment dyes affect the material's dielectric properties because the pigment itself has its own dielectric properties.

Other than that, it appears that as frequency increases, the relative permittivity tends to decrease slightly. Interestingly, a study conducted at $1 - 100\text{MHz}$ [8] found that PLA has the lowest relative permittivity and PETG the highest, while another study at the W-Band ($75 - 110\text{GHz}$) [3] reported that PLA exhibit the highest relative permittivity and PETG the lowest. This suggests that at higher frequencies, the decline in relative permittivity may become more gradual, with each material potentially showing different rates of changes. This variability could be due to the challenges of accurately measuring the dielectric properties of a material, particularly when the properties are highly dependent on various factors, as mentioned earlier. Moreover, the two studies used different measurement techniques, which are necessary for different frequency ranges, and this may have contributed to the observed discrepancies.

3 Setup and Limits

3.1 Test setup and parameters

A 4-Port VNA, in this case Rohde & Schwarz ZNB8 VNA, in combination with the standardized test board from FTZ Zwickau (Figure 3.1a) and a custom made fixture for the test board are used to measure the mixed-mode S-Parameters of the CMC, as illustrated in Figure 3.2. A Shin-Etsu gold foil (Figure 3.1b) is also required, it "consists of parallel rows of gold-plated brass wires in a silicon rubber sheet" [12]. The foil is very thin yet durable and flexible, designed to establish a low resistance ($< 0.1\Omega$ [12]) electrical connection between the CMC and the PCB while maintaining minimal pressure. This low resistance connection reduces energy loss as heat, resulting in a more efficient connection. To minimizes the risk of electrostatic discharge (ESD) that could potentially damage sensitive electronic components, the gold foil is held in place with an ESD tape, which is specially designed to minimize the electro static charge produced during unwinding and application. Furthermore, the custom made 3D printed fixture is designed using Autodesk Fusion 360, then sliced with Ultimaker Cura and printed using Ultimaker 3.



(a) Without gold foil

(b) With gold foil

Figure 3.1: CMC test board

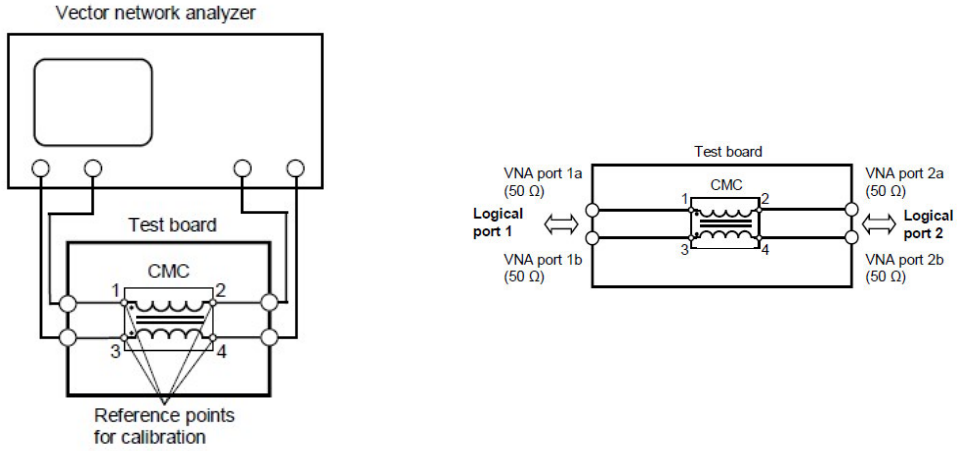


Figure 3.2: Test setup for S-Parameter measurements [2]

3.1.1 3D design, slicing and printing

The first step is to design the fixture. Autodesk Fusion 360 is ideal for this task, as it allows for designing multiple component in one file, direct adjustments to the fixture's dimensions at any time, and provides access to the process history. After the design is finished, the file needs to be exported as type Stereolithography (.stl) so it can be processed using a slicing software, in this case Ultimaker Cura. The slicing software then converts the STL format into a G-Code, which consists of commands for the 3D printer. The slicer also allows adjustments to the printer settings such as printing temperature, infill density, infill pattern, print speed and many more. Research has shown that filling pattern and density influence the relative dielectric properties of the 3D print [5]. However, due to the narrow and thin nature of the prints in this study, these factors do not significantly impact the results. The prints are so narrow that they cannot utilize any pattern or be made less dense. To avoid errors, it's important to select the correct type of filament in the slicing software to ensure the correct print settings are applied for the selected material.

The printer being used, which is Ultimaker 3, has two extruders with a 0.4mm nozzle. It is important to either use the same type of filament in both extruders or disable one extruder in the slicing software to prevent the use of different temperatures for melting the filament, as each filament requires a specific melting temperature. For instance, if PLA and ABS filaments are used together, the printer will default to the higher temperature

needed for ABS, which is too high for PLA. The higher temperature makes the PLA's viscosity too low, increasing the likelihood of printing failure.

3.1.2 Test fixtures design

Previously, only a clamp was used to hold the CMC in place, displayed in Figure 3.3. However, this method proved insufficient because it ensured neither consistent placement nor reliable contact. Even a slight variation in positioning of the CMC could result in different measurement outcomes.



Figure 3.3: The initial state

Two other designs were developed and evaluated, before the final design was reached. The first version, illustrated in Figure 3.4, featured a bottom piece to hold the CMC in place to eliminate horizontal movement, with a top piece that clamped onto the sides of the PCB and applied downward pressure using a nylon screw. However, this design proved ineffective due to excessive number of moving components, which complicated its use and resulted in undefined pressure, leading to inconsistency in the results.

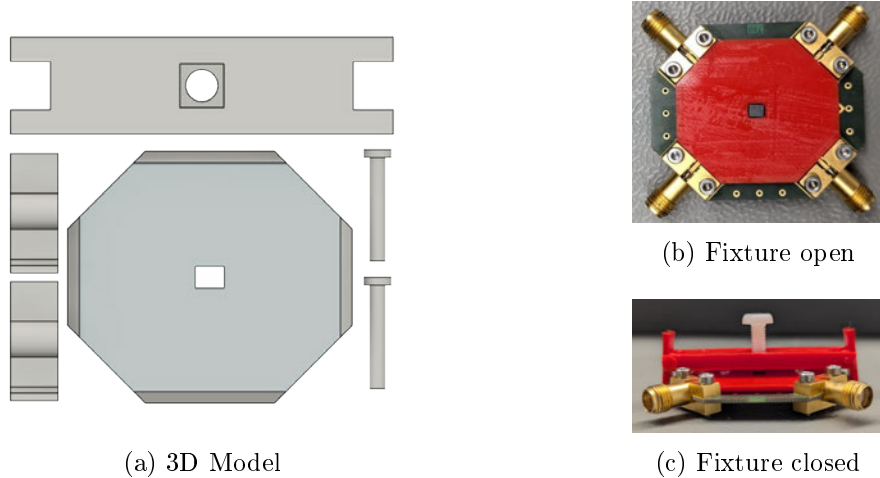


Figure 3.4: First version

The second version, depicted in Figure 3.5, incorporates a clip function for ease of use. This fixture consists of two parts: the bottom part holds the CMC in place, while the top part features a central pillar that applies downward mechanical pressure on the CMC to establish contact with the PCB. Both parts are connected with a hinge.

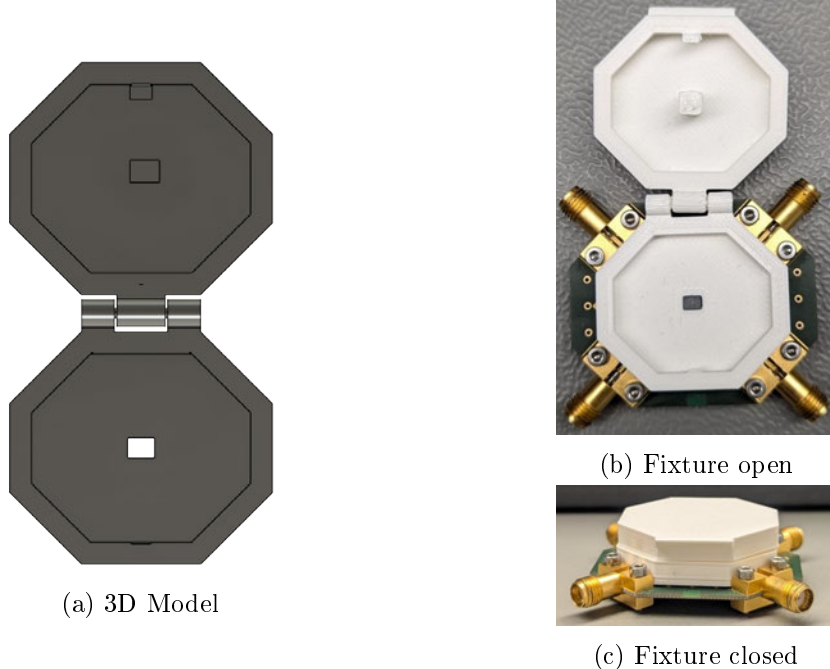


Figure 3.5: Second version

Because the fixture was not in any way fixed on the PCB, the fixture had some vertical movement which could cause undefined pressure and therefore not yet suitable as a final design.

The final design, as seen in Figure 3.6, is an improvement from the second version. It is secured in place with side wings that are screwed down to a piece positioned below the PCB, eliminating vertical movement ensuring that adequate and constant pressure is applied to the CMC. Skeletonizing the inlay offers advantages such as reduced printing time and filament conservation. The inlay is removable, allowing the CMC to easily be taken out without dismantling the entire fixture. Additionally, the removable inlay enables convenient replacement or repositioning of the gold foil.

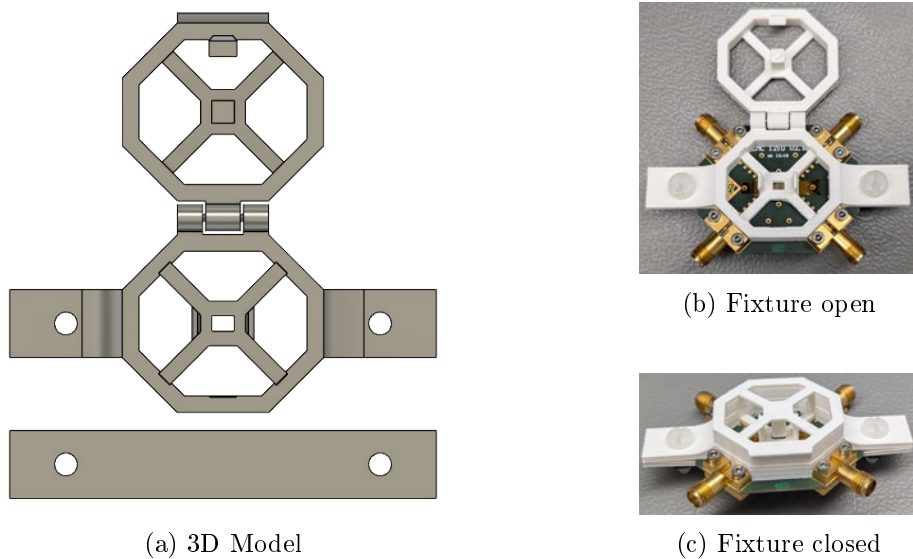


Figure 3.6: Final version

3.2 Recommended limits

To evaluate mixed-mode S-Parameters for the 4-port board, the Open Alliance recommends adhering to the limits for each parameter as shown in the following figures.

$$RL \geq \begin{cases} 27 & 1 \leq f \leq 10 \\ 27 - 9.75 \log\left(\frac{f}{10}\right) & 10 \leq f \leq 66 \end{cases} \text{ dB, frequency } f \text{ in MHz}$$

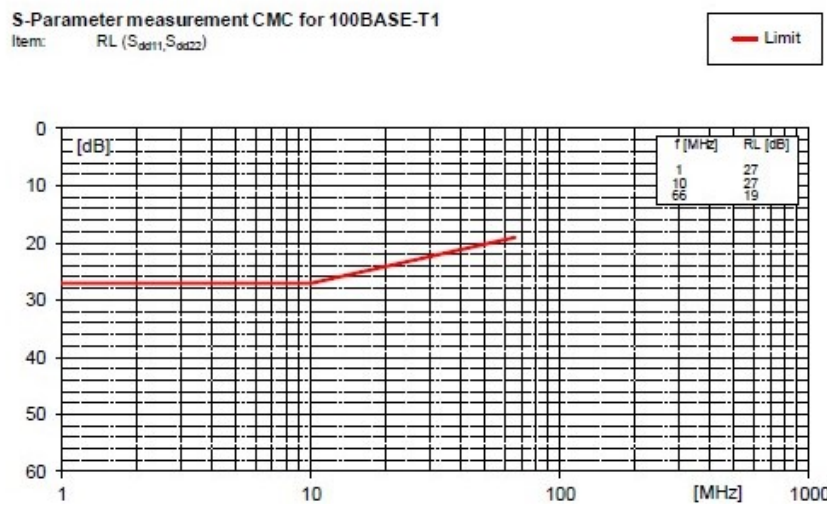


Figure 3.7: Recommended limit for S_{dd11} and S_{dd22} (RL) [2]

3 Setup and Limits

$$IL \leq \begin{cases} 0.5 & 1 \leq f \leq 10 \\ 0.5 + 0.39 \log\left(\frac{f}{10}\right) & 10 \leq f \leq 33 \\ 0.8 + 1.00 \log\left(\frac{f}{33}\right) & 33 \leq f \leq 66 \end{cases} \text{ dB, frequency } f \text{ in MHz}$$

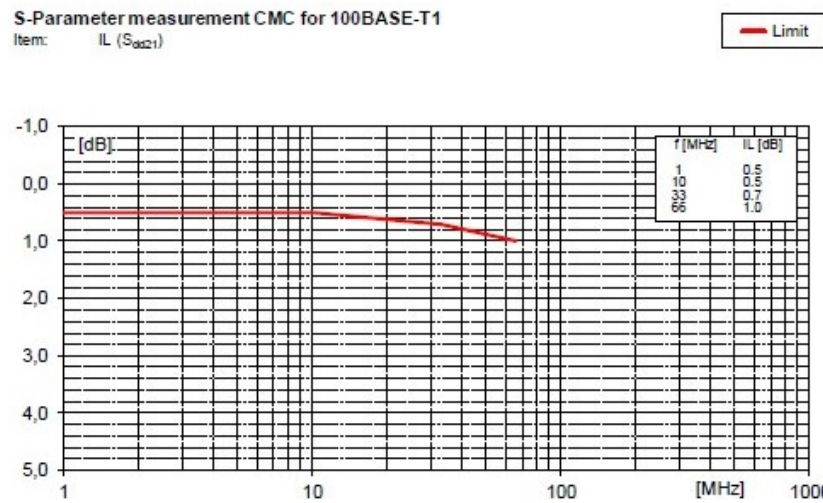


Figure 3.8: Recommended limit for S_{dd21} (IL) [2]

$$CMR \geq \begin{cases} 25 + 20 \log\left(\frac{f}{1}\right) & 1 \leq f \leq 10 \\ 45 & 10 \leq f \leq 80 \\ 45 - 20 \log\left(\frac{f}{80}\right) & 80 \leq f \leq 200 \end{cases} \text{ dB, frequency } f \text{ in MHz}$$

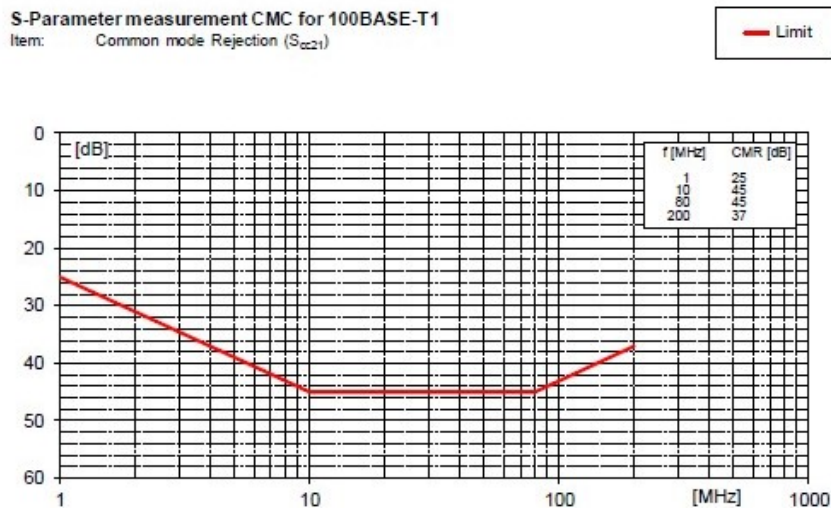


Figure 3.9: Recommended limit for S_{cc21} (CMR) [2]

4 Test execution and evaluation

4.1 Calibration

Before the measuring process can begin, the VNA must be calibrated using the parameters listed in Table 4.1 and a standardized calibration board from FTZ Zwickau (Figure 4.1) for the Through, Open, Short, Match (TOSM) calibration. This step is crucial to ensure that the VNA cable and the test board do not interfere with the CMC measurement, also minimize any uncertainty and/or errors to an acceptable level.

Parameter	Value
Sweep f_{Start}	300 kHz
Sweep f_{Stop}	1 GHz
Sweep type	Logarithmic
Sweep points	1600
Output power	minimum -10 dBm
Measurement bandwidth	100 Hz
Logic Port Impedance Differential Mode	100 Ω
Logic Port Impedance Common Mode	25 Ω
Data calibration kit (VNA)	used kit for calibration
Averaging function	16 times
Smoothing function	deactivated

Table 4.1: Calibration parameters [6]

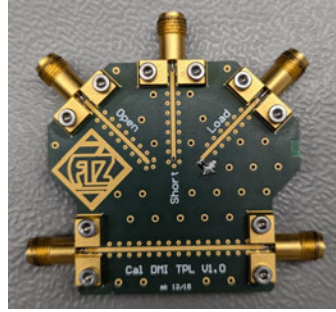


Figure 4.1: Calibration board

To achieve higher accuracy, it is recommended to allow the VNA to warm up for at least 30 minutes before calibration or use [9][10]. Due to the high number of sweep points and the averaging factor required for accuracy, this calibration process takes approximately four hours to complete.

4.2 Measurement and evaluation

After the calibration is finished, the measurement process can begin to determine the optimal fixture configuration for characterizing the CMC. These processes involved several steps: first, adjust the pressure applied to the CMC; then, a comparison was made between the skeletonized and full-body inlays; next, select the best material for the fixture; subsequently, check if the results are repeatable; and finally, compare the test results of the CMC using the fully configured fixture to those of a soldered CMC on a PCB. Even though the data sheet states that the CMC has no polarity (see Figure 2.1c), it's important to ensure that the CMC is oriented correctly, with the writing on the CMC facing in a readable direction, as improper orientation does affect the measurement results.

4.2.1 Mechanical pressure

After the design was completed, the first step was to achieve optimal and constant pressure on the CMC to ensure sufficient contact with the PCB while avoiding excessive pressure that could damage the CMC. The test involved adjusting the height of the pillar intended to apply pressure on the CMC, using the following heights: 72mm, 73mm, 74mm and 75mm.

4 Test execution and evaluation

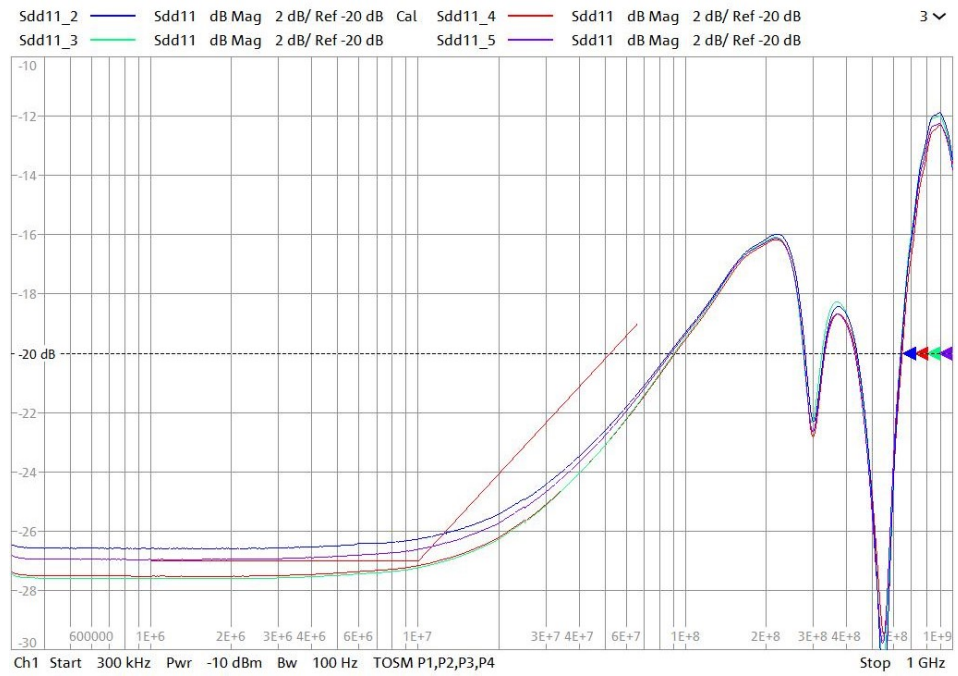


Figure 4.2: Pressure test - S_{dd11}

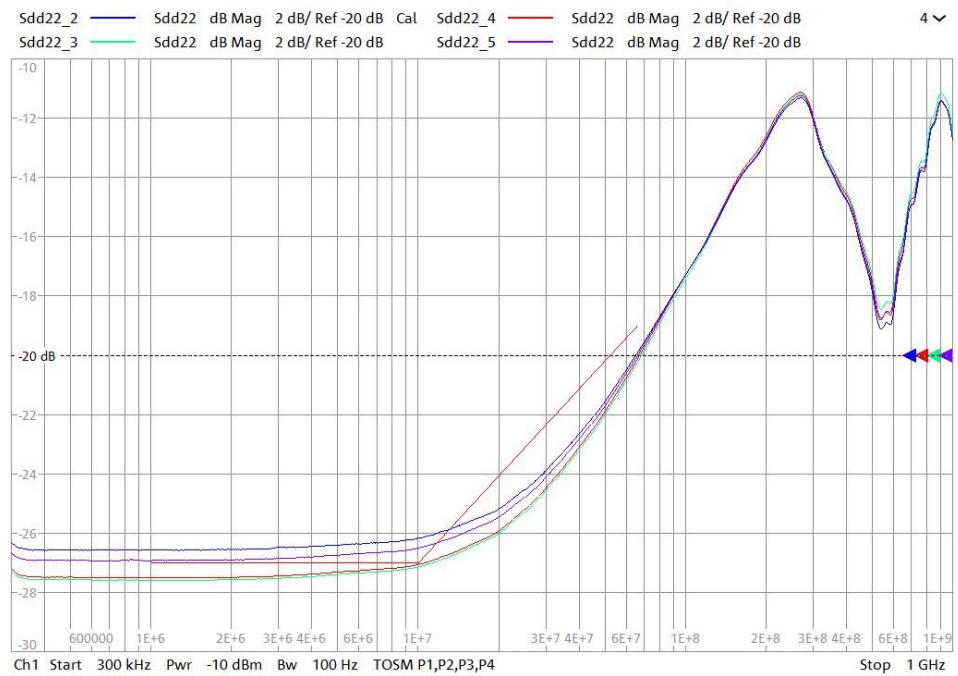


Figure 4.3: Pressure test - S_{dd22}

4 Test execution and evaluation

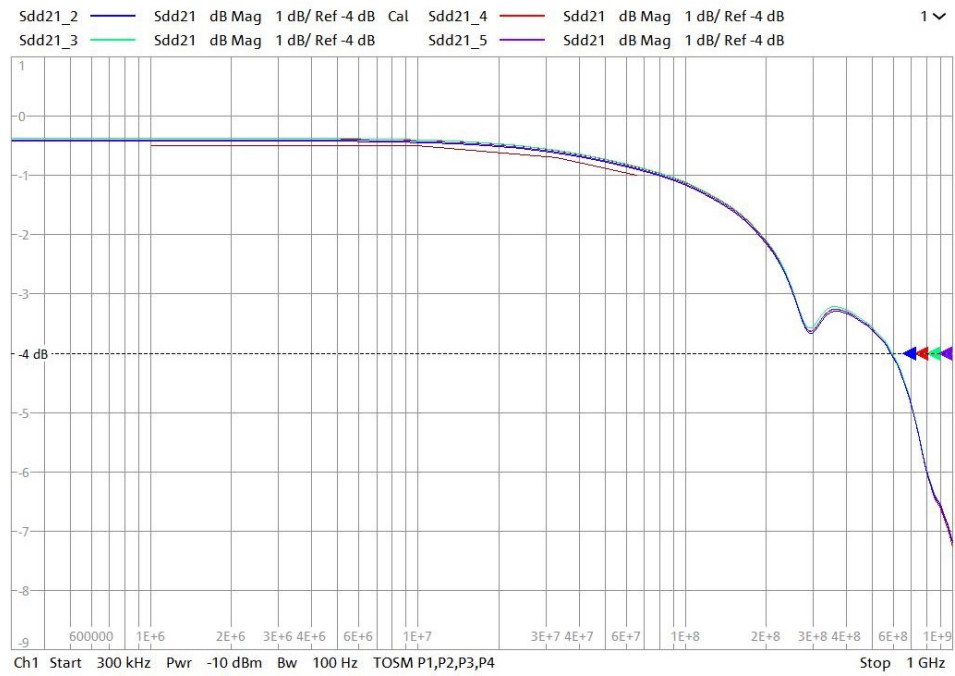


Figure 4.4: Pressure test - S_{dd21}

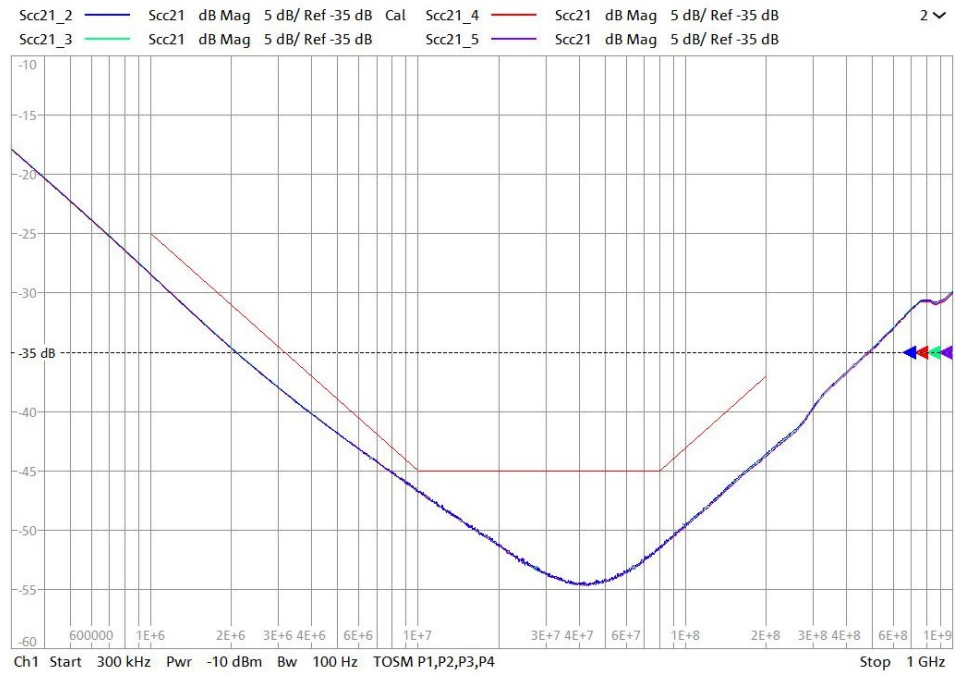


Figure 4.5: Pressure test - S_{cc21}

The *72mm* (blue) and *75mm* (purple) pillars did not meet the recommended limit for return loss at lower frequencies, as shown in Figure 4.2 and 4.3, and were therefore excluded. The *72mm* pillar did not provide enough pressure on the CMC, while the *75mm* pillar applied excessive pressure. The *73mm* (turquoise) pillar was selected for further use because it performed slightly better than the *74mm* (red) pillar, as indicated in the figures above. Make sure to change or reposition the gold foil after several use, because of wear and tear (see Figure 3.1b), which can alter the measurement results.

4.2.2 Inlay

As previously mentioned, testing both the skeletonized and full-body inlay designs is necessary to determine if there is any noticeable difference in performance.

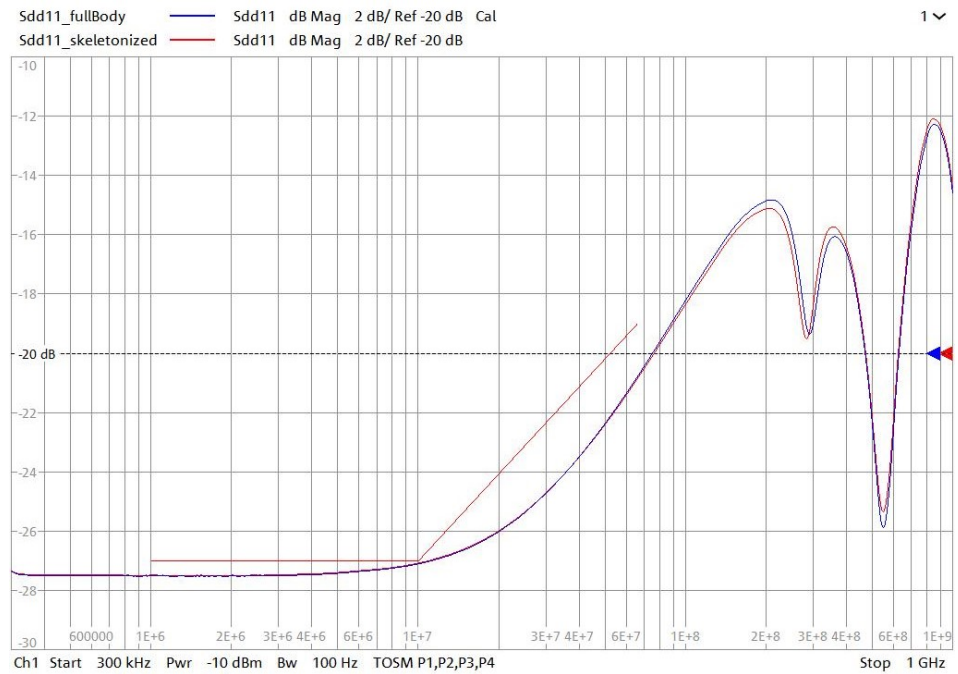


Figure 4.6: Inlay test - S_{dd11}

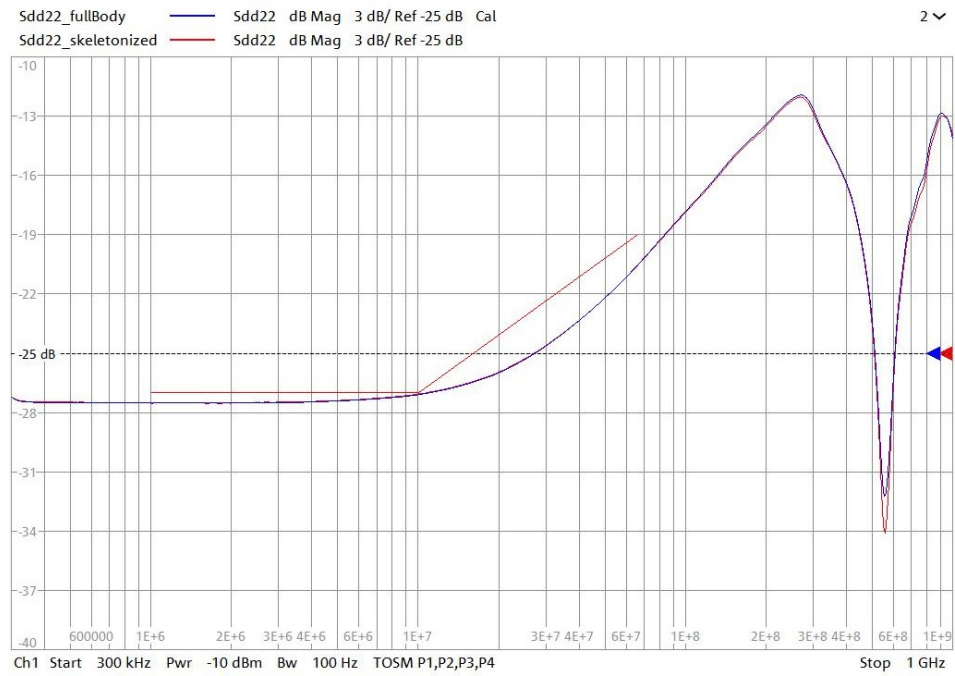


Figure 4.7: Inlay test - S_{dd22}

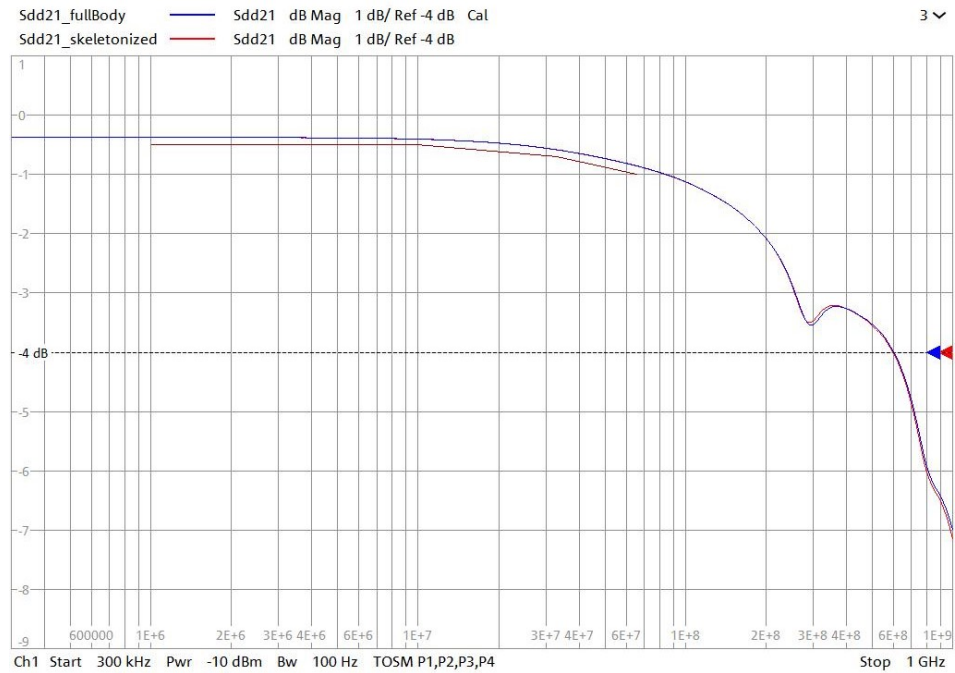


Figure 4.8: Inlay test - S_{dd21}



Figure 4.9: Inlay test - S_{cc21}

There is minimal deviation in S_{dd11} and S_{dd22} measurements between the two designs. The skeletonized inlay performs slightly better at higher frequencies, although the difference is not significant. As a result, the decision was made to proceed with the skeletonized inlay to reduce printing time and conserve material.

4.2.3 Material

This test aims to select the most suitable material for the fixture from the three chosen filaments: white PLA, transparent PETG and black ABS. These materials were selected because they are among the most popular and readily available materials on the market. Additionally, they are the most researched in terms of relative permittivity.

4 Test execution and evaluation

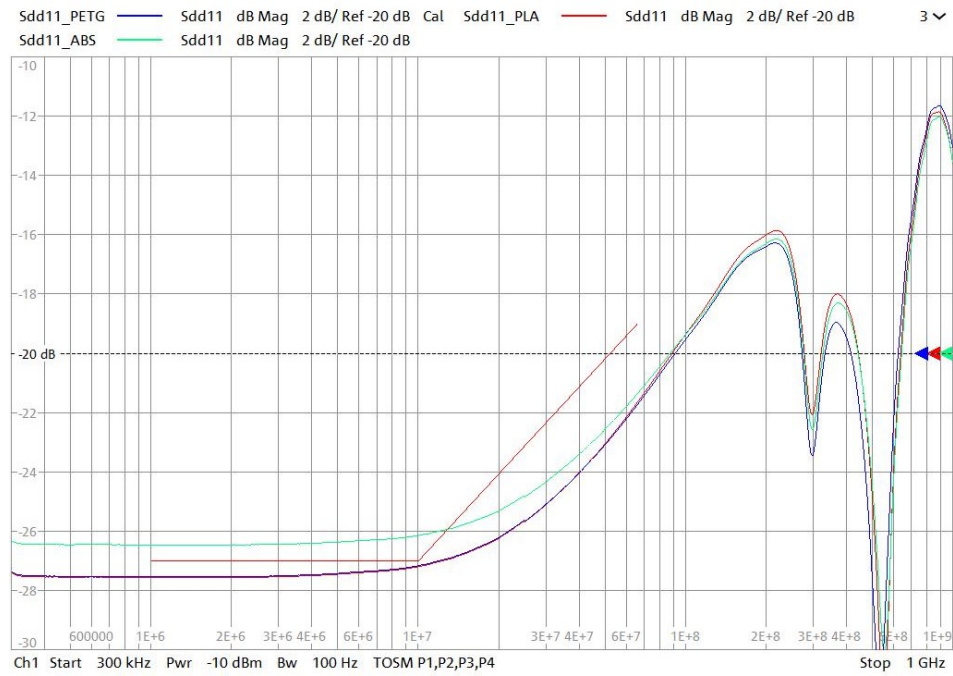


Figure 4.10: Material test - S_{dd11}

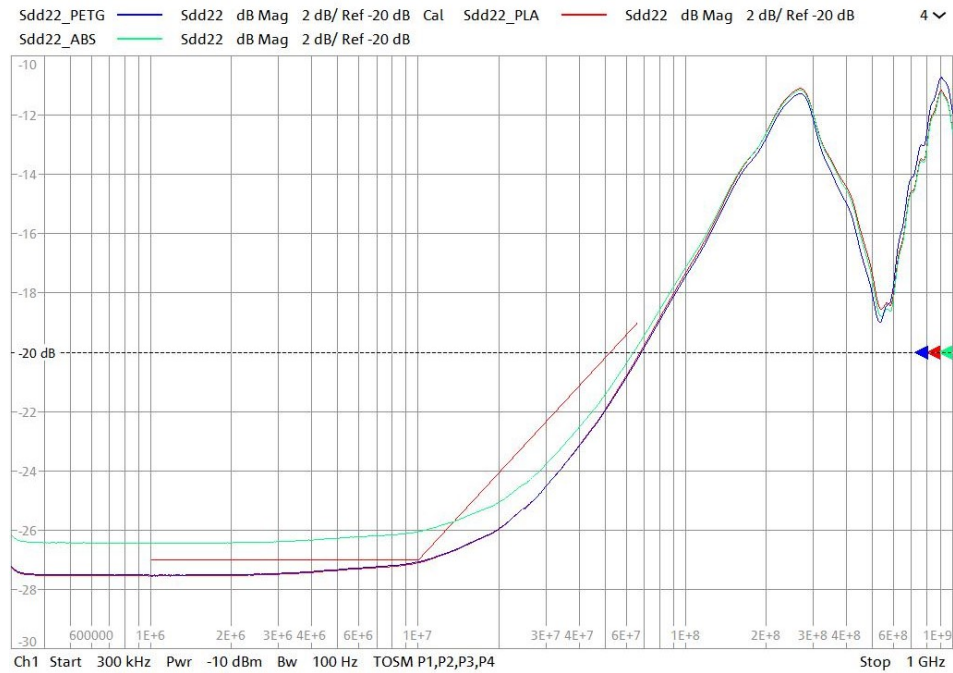


Figure 4.11: Material test - S_{dd22}

4 Test execution and evaluation

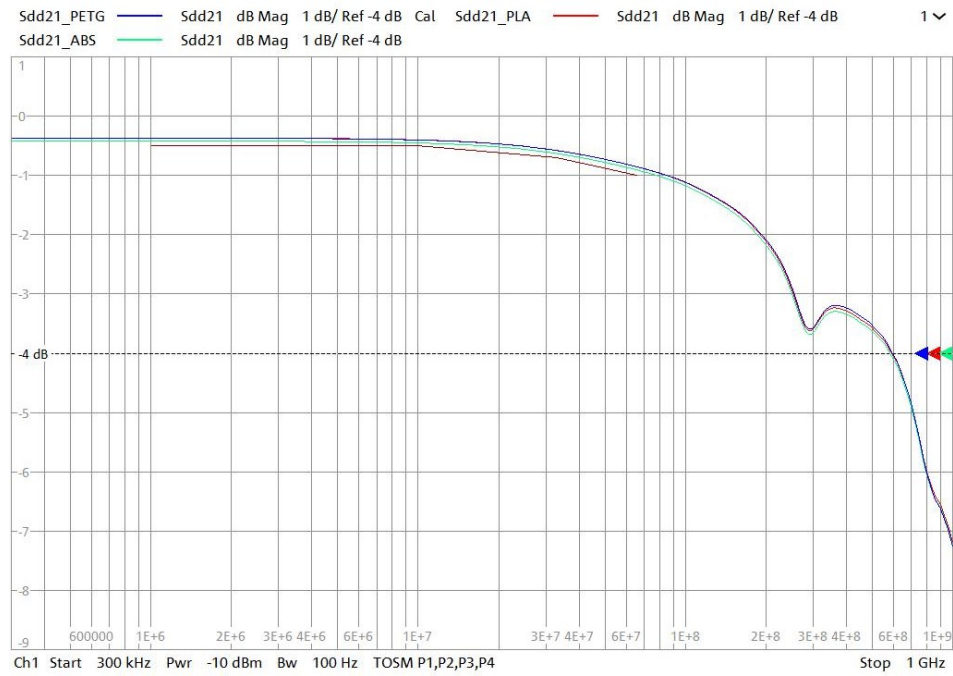


Figure 4.12: Material test - S_{dd21}

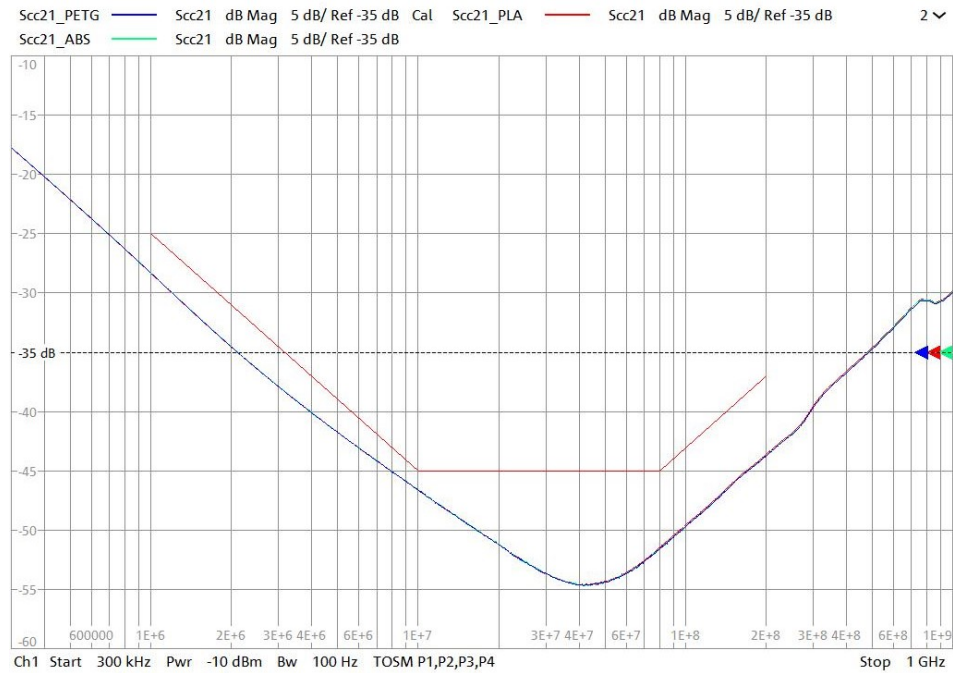
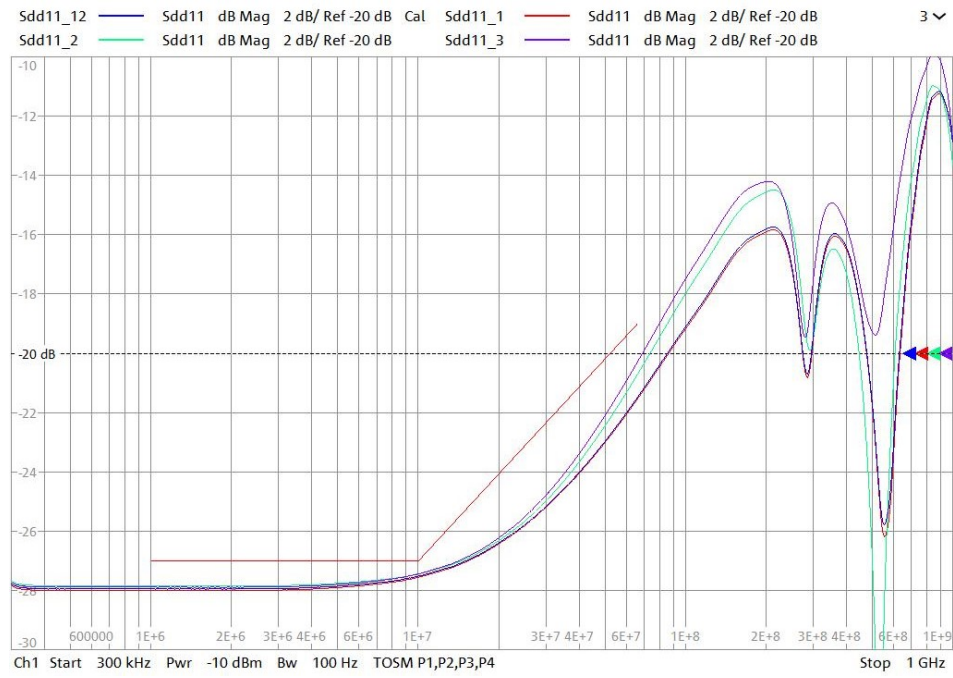


Figure 4.13: Material test - S_{cc21}

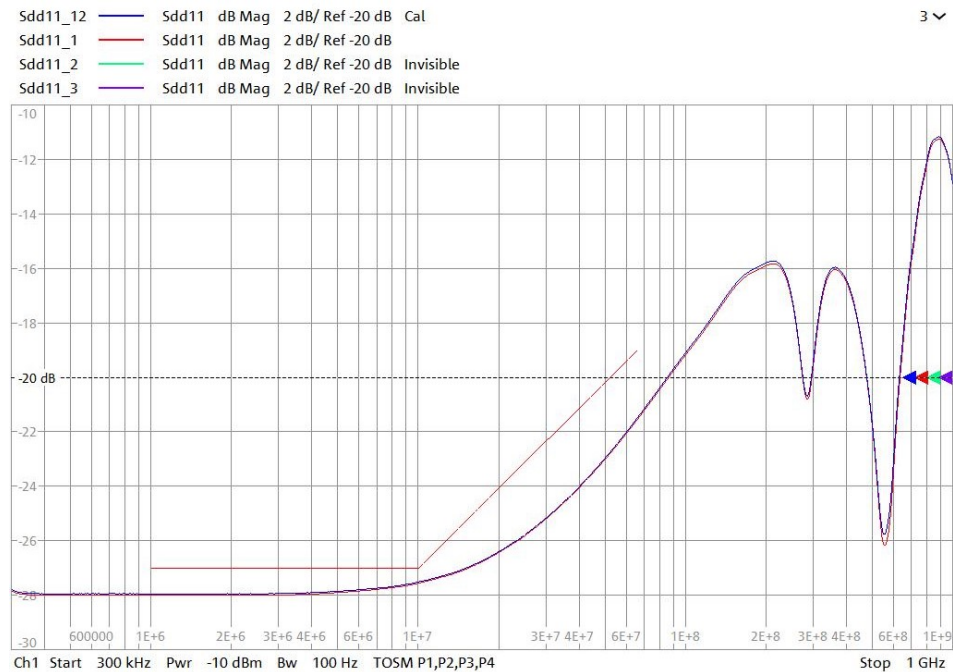
As observed from the measurements, both PLA (red) and PETG (blue) passed all tests, whereas ABS (turquoise) did not. It is expected that PLA would have the lowest relative permittivity among the three chosen filaments at these frequencies. However, PETG showed unexpectedly similar result to PLA. This may be because PETG chosen was transparent, which typically results in lower relative permittivity compared to colored materials [7]. Additionally, as mentioned in section 2.3.1, PETG had the lowest relative permittivity at higher frequencies, likely because PETG's dielectric properties are more frequency dependent compared to PLA. Ultimately, PLA was chosen because PETG proved more difficult to print with and was not as strong as anticipated. The PETG broke when attempting to remove the inlay, possibly due to improper storage of the filament, which can absorb moisture from the air and become brittle. As it is known, PETG is particularly sensitive to moisture.

4.2.4 Validation

For this test, three different samples were measured in the following sequence: Sample 1, Sample 2, Sample 3 and then Sample 1 again to determine if the fixture can produce repeatable results.

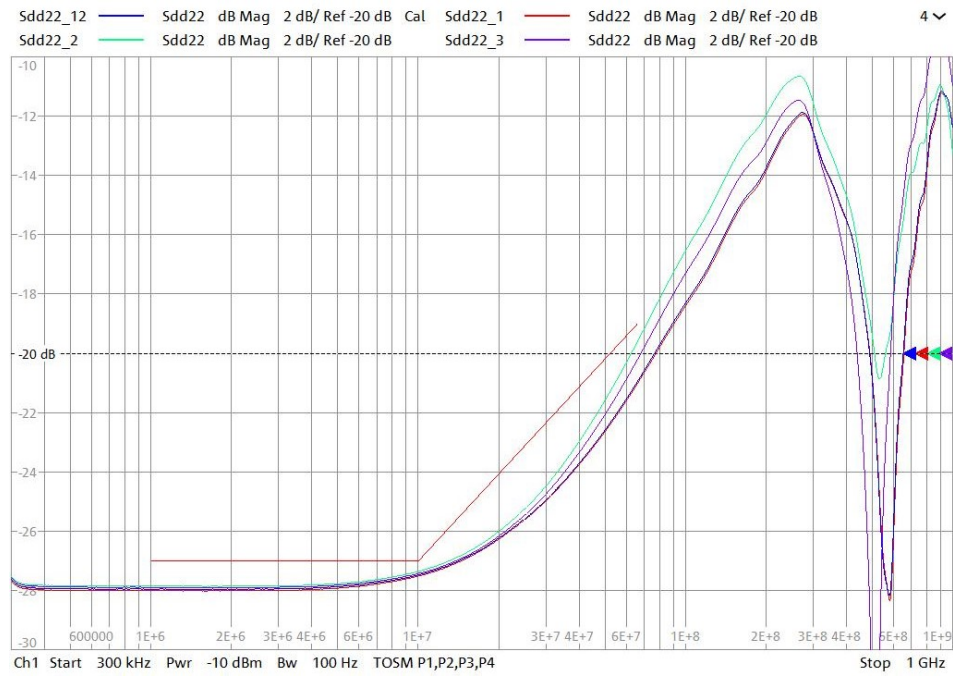


(a) All samples used in the test

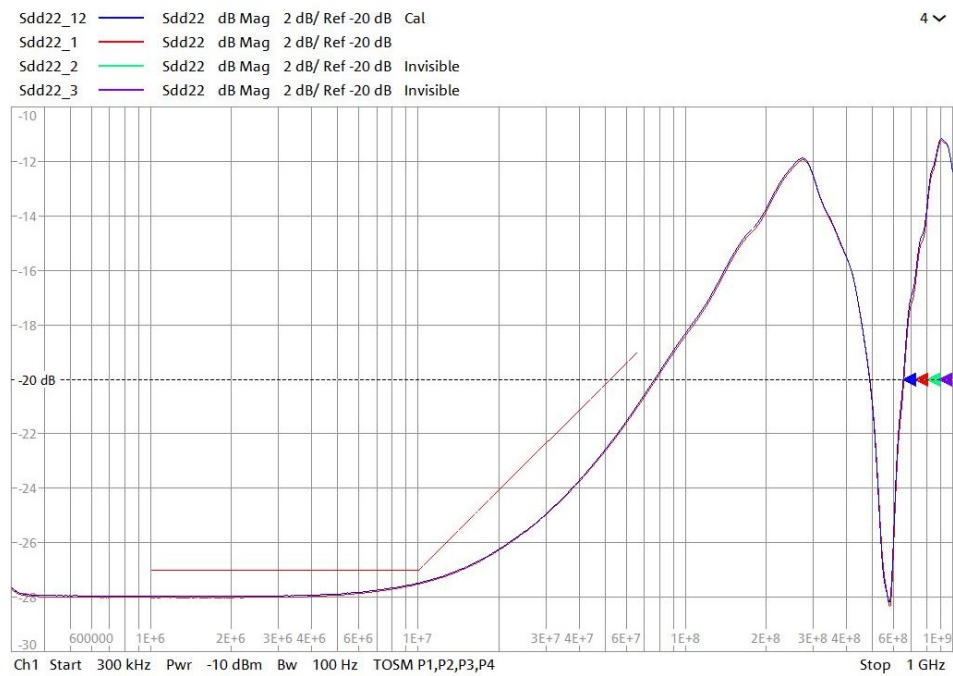


(b) Sample 1 before and after the measurement of Sample 2 and Sample 3

Figure 4.14: Validation test - S_{dd11}



(a) All samples used in the test

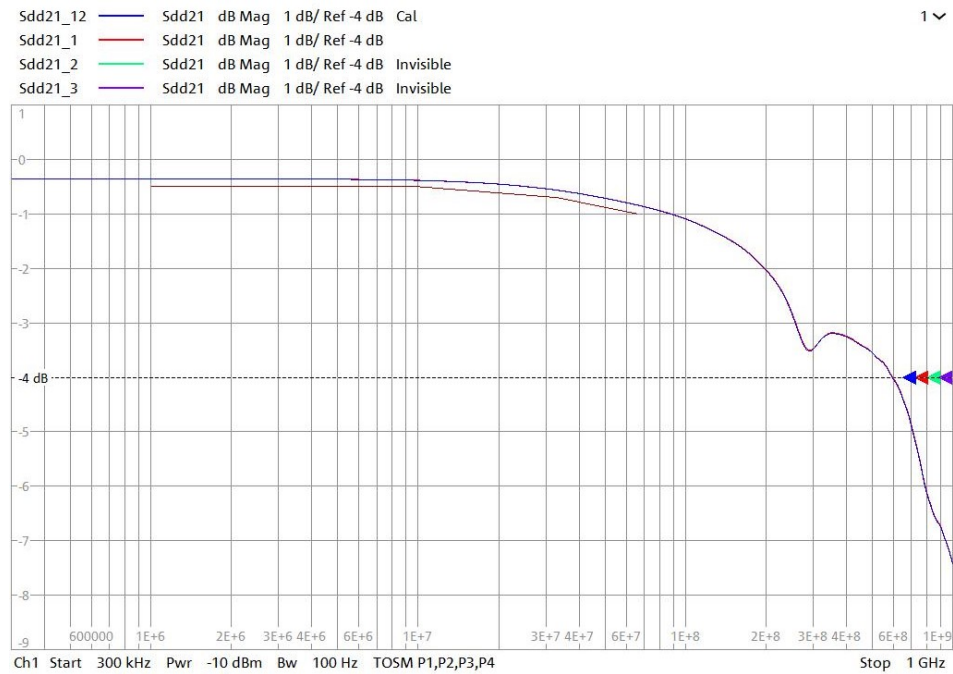


(b) Sample 1 before and after the measurement of Sample 2 and Sample 3

Figure 4.15: Validation test - S_{dd22}

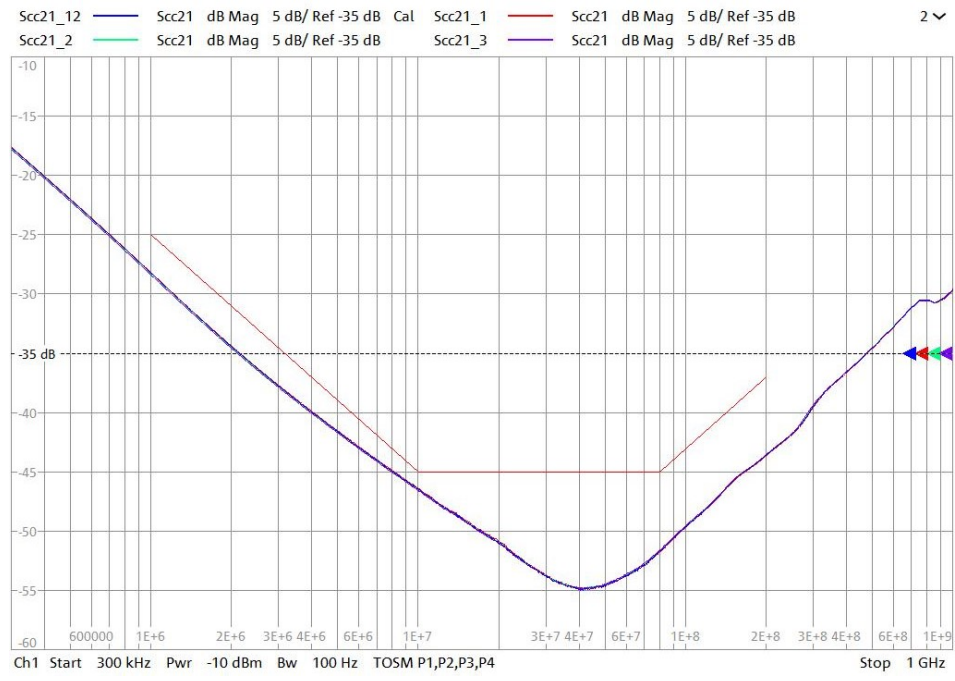


(a) All samples used in the test



(b) Sample 1 before and after the measurement of Sample 2 and Sample 3

Figure 4.16: Validation test $-S_{dd21}$



(a) All samples used in the test



(b) Sample 1 before and after the measurement of Sample 2 and Sample 3

Figure 4.17: Validation test - S_{cc21}

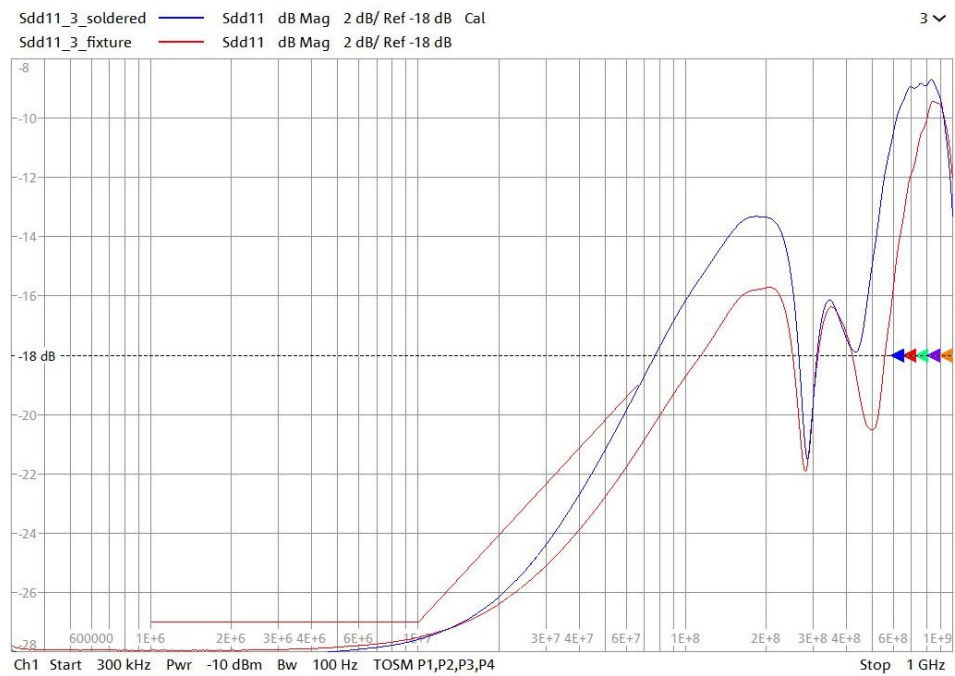
It is typical for different CMC samples to have varying measurements due to production imperfections, meaning the CMCs are not 100% identical. This makes it essential to measure the CMC before deployment. All measurements remained within the recommended limits. Moreover, the measurements for Sample 1, taken before (red) and after (blue) testing Sample 2 (turquoise) and Sample 3 (purple) remained consistent for all parameters, indicating a reliable setup.

4.2.5 Verification

To verify the fixture's intended design and functionality, the CMC was first measured using the fully configured fixture, then the same CMC was soldered to a PCB and measured again for comparison. The DC resistance of the soldered CMC was measured with a multimeter to confirm that a proper connection was established, which showed a resistance of approximately 5Ω . This process was repeated with another sample to ensure statistical reliability.

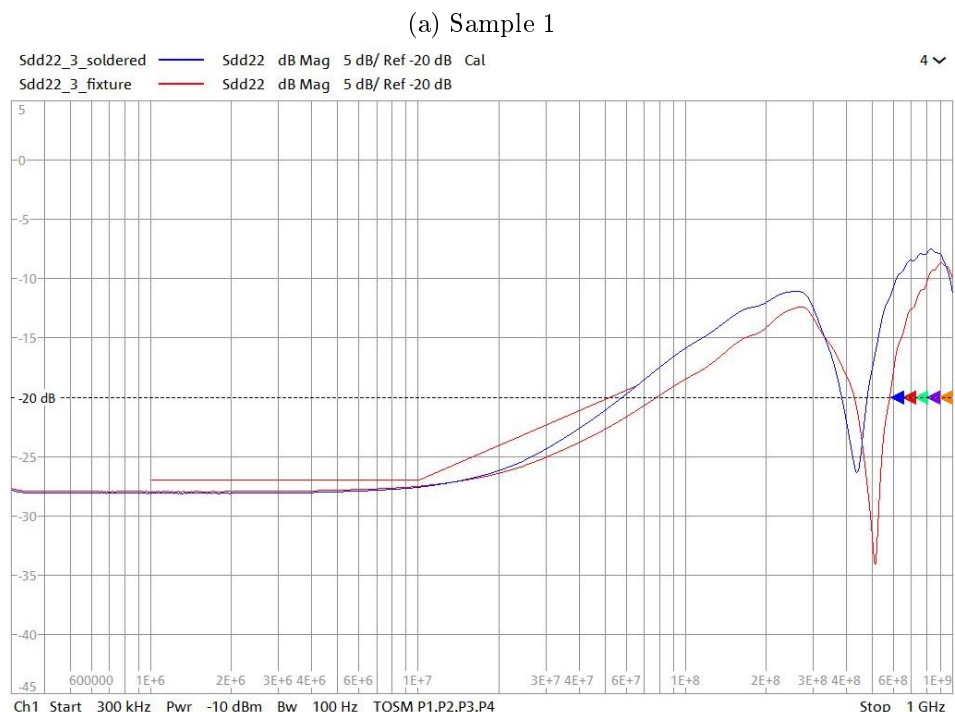
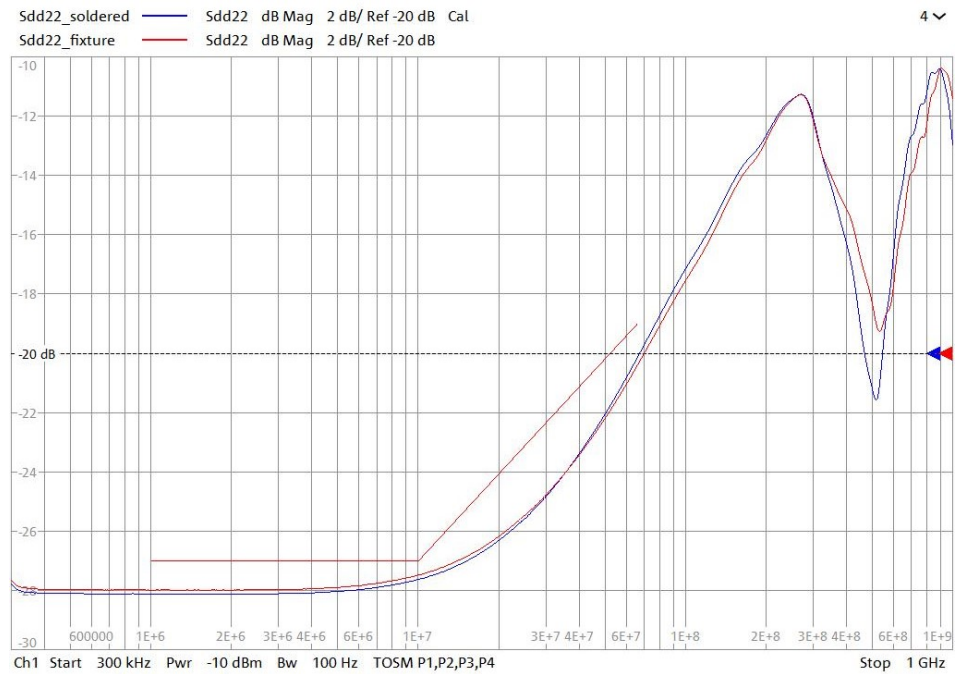


(a) Sample 1



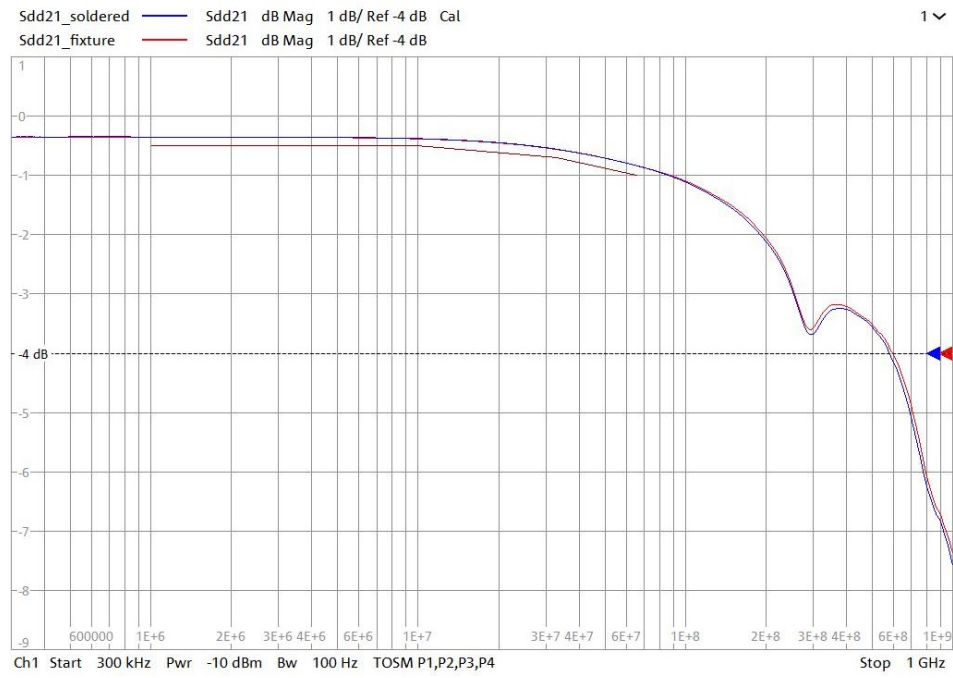
(b) Sample 2

Figure 4.18: Verification test - S_{dd11}

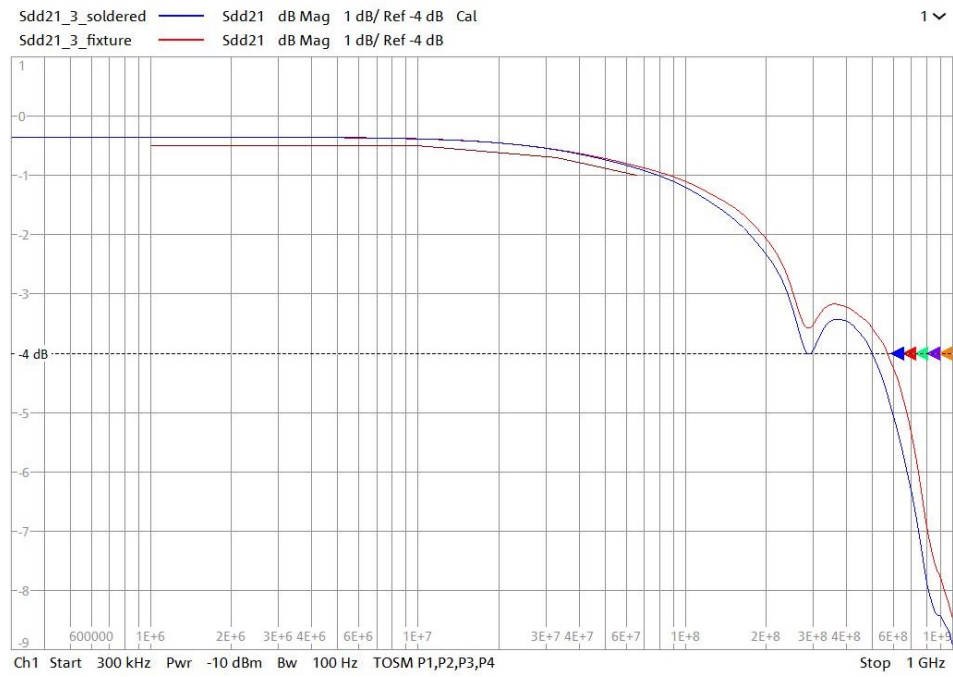


(b) Sample 2

Figure 4.19: Verification test - S_{dd22}



(a) Sample 1

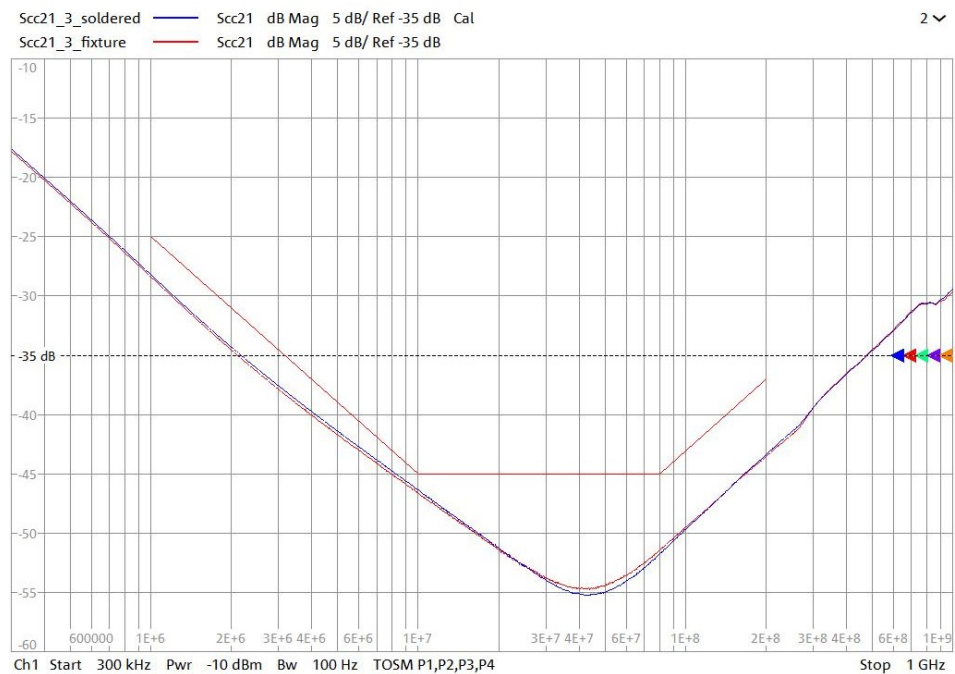


(b) Sample 2

Figure 4.20: Verification test - S_{dd21}



(a) Sample 1



(b) Sample 2

Figure 4.21: Verification test - S_{cc21}

Noticeable deviations were observed in S_{dd11} and S_{dd22} for both sample 1 and 2 at higher frequencies, which represent the return loss. Since a higher RL indicates better device performance, the fixture with the gold foil yielded superior results compared to the soldered connections. A more subtle deviations were also observed in S_{dd21} and S_{cc21} , further indicating that the fixture performs better than the soldered configuration. This could be attributed to the inconsistency of soldering. Particularly at high frequencies, excess solder can disrupt impedance continuity, leading to impedance jumps. In contrast, the gold foil offers high conductivity and ensures a direct, low-resistance connection, thereby improving measurement accuracy and consistency.

5 Conclusion and future work

Due to production imperfections, even CMCs of the same model may exhibit slightly different characteristics, especially at higher frequencies, as shown in section 4.2.4. This is why it's essential to characterize each CMC before deployment to ensure optimal performance. The CMC is a small and fragile component, and the soldering and desoldering process is unsustainable as it can damage the CMC or alter its physical traits, potentially changing its characteristics. To address this issue, a solution was developed: a solderless 3D-printed fixture that sits on top of the PCB and securely holds the CMC in place, while a gold foil is used to establish a better connection between the PCB and CMC.

The optimal configuration for the fixture at these frequencies (300kHz - 1GHz) includes using PLA as the material due to its ability to provide the best results among all tested materials, along with its ease of printing and overall robustness. While the results are acceptable, future experiments could explore using different colors, possibly transparent, since research suggest that colorless materials tend to have lower permittivity [7]. Besides, PETG should be reconsidered for use if higher frequency testing is needed, as research indicates that PETG may perform better at higher frequencies [3].

On top of that, a *73mm* pillar height is ideal for applying sufficient pressure to ensure sufficient contact between the CMC and the PCB. Additionally, a skeletonized body design is used to reduce printing time and conserve material. Lastly, the fixture is securely fixed in place to eliminate any movement, ensuring stability during measurements.

Reflecting on the development process, the design and precise measurement of the test board dimensions took the most time, as there were no existing data on the board's dimensions available. The fixture needed to be made-to-measure to ensure a perfect fit and eliminate any movement that could affect the accuracy of the results.

This project is considered successful, as the fixture is easy to use, reliable, and produces better results than traditional soldering. It also provides a foundation for future development of similar components and testing setups, with the configurations and method-

ologies from this thesis adapted to accommodate the new forms. For instance, the 3-port board [2] used for further characterizing the CMC would also require a fixture, or larger CMCs could be tested on the 4-port board, necessitating adaptations to the inlay design. Furthermore, the fixture could be directly fixed to the test board, making the setup more compact, further reducing printing time and material usage.

Bibliography

- [1] ALAMIN, A. (ABRACON, LLC): Common Mode Chokes Basics and Applications. (2022). – URL <https://abracon.com/uploads/resources/Common-Mode-Chokes-Basics-and-Applications.pdf>
- [2] DR. B. KÖRBER (FTZ ZWICKAU): 100BASE-T1 EMC Test Specification for Common Mode Chokes. 2.0 (2020). – URL https://opensig.org/wp-content/uploads/2024/01/OA-1000Base-T1_CMC-Test-Specification-v2.0.pdf
- [3] GREGORY, N.: Measuring the Electrical Properties of 3D Printed Plastics in the W-Band. In: *Electrical Engineering Undergraduate Honors Theses* (2022). – URL <https://scholarworks.uark.edu/eleguht/85/>
- [4] HAYT, W. H. ; BUCK, J. A.: Engineering Electromagnetics; 8th ed. (2011). ISBN 978-0-073-38066-7
- [5] KATTEL, B. ; HUTCHCRAFT, W. E. ; GORDON, R. K.: Exploring Infill Patterns on Varying Infill Densities on Dielectric Properties of 3D Printed Slabs. In: *2023 Antenna Measurement Techniques Association Symposium (AMTA)* (2023), S. 1–5. – ISSN 2474-2740
- [6] KIRCHMEIER, T. (BMW AG) ; JANKER, G. (RUETZ SYSTEM SOLUTIONS GMBH) ; ALL MEMBERS OF THE OPEN ALLIANCE TC8 WORKING GROUP: OPEN Alliance Automotive Ethernet ECU Test Specification Layer 1. 3.0 (2020). – URL https://opensig.org/wp-content/uploads/2024/01/OA_Automotive_Ethernet_ECU_TestSpecifications_Version_3.0.zip
- [7] PICHA, T. ; PAPEZOVA, S. ; PICHA, S.: Evaluation of Relative Permittivity and Loss Factor of 3D Printing Materials for Use in RF Electronic Applications. In: *Processes* 10 (2022), Nr. 9. – ISSN 2227-9717

Bibliography

- [8] PÍCHA, T. ; PAPEŽOVÁ, S.: Dielectric properties of materials for 3D printing at high frequencies. In: *Research in Agricultural Engineering* 69 (2023), Nr. 1, S. 28–35. – ISSN 12129151
- [9] ROGERS, A. E. E. (MASSACHUSETTS INSTITUTE OF TECHNOLOGY): Automated tests of VNA warm-up needed for highest accuracy. (2021). – URL https://www.haystack.mit.edu/wp-content/uploads/2021/06/memo_EDGE_S_363.pdf
- [10] ROHDE&SCHWARZ: R&S ZNB Vector Network Analyzer Specifications. 07.00 (2023). – URL https://scdn.rohde-schwarz.com/ur/pws/dl_downloads/pdm/cl_brochures_and_datasheets/specifications/3608_3278_22/ZNB_specs_en_3608-3278-22_v0700.pdf
- [11] RYDER, B.: The 3D Printing Holy Trinity: PLA, ABS, and PETG. . – URL https://www.sliceengineering.com/blogs/news/the-3d-printing-holy-trinity?srsltid=AfmBOoprTd8x1MC7axxfnU3KL5_jsIXD3_MnC7Cr_Jec_9-phFEC1naw
- [12] SHIN-ETSU POLYMER Co, LTD.: Shin-Etsu Inter-Connector MT series. . – URL <https://www.shinetsu.info/product/mt-type-of-inter-connector/>
- [13] TDK CORPORATION: TDK ACT1210L-201-2P-TL00. (2022). – URL https://product.tdk.com/en/search/emc/emc/cmf_cmc/info?part_no=ACT1210L-201-2P-TL00
- [14] TELEDYNE LECROY, INC.: Introduction to Mixed-Mode S-parameters. (2021). – URL <https://blog.teledynelecroy.com/2021/05/introduction-to-mixed-mode-s-parameters.html>

A Appendix

A.1 Tools and Equipment

Table A.1 lists the tools and equipment used when working on the topic of the Bachelor thesis.

Table A.1: Tools and equipment

Tool/Equipment	Use
Autodesk Fusion 360	Software to design 3D Fixtures
Ultimaker Cura	Slicing software for printing 3D Fixtures
Ultimaker 3	3D Printer to print the fixtures
Rhode & Schwarz ZNB8	Vector Network Analyzer to measure the S-parameters
FTZ calibration board	TOSM calibration for the VNA
FTZ test board	Board to connect the CMC to the VNA
Shin-Etsu gold foil	Gold foil placed between CMC and PCB to create an electrical contact
Multimeter	Tool for measuring voltage, current, and resistance in circuits

Erklärung zur selbständigen Bearbeitung

Hiermit versichere ich, dass ich die vorliegende Arbeit ohne fremde Hilfe selbständig verfasst und nur die angegebenen Hilfsmittel benutzt habe. Wörtlich oder dem Sinn nach aus anderen Werken entnommene Stellen sind unter Angabe der Quellen kenntlich gemacht.



Ort

Datum

Unterschrift im Original